Entanglement Spacing Variability in Polystyrenes with Narrow Molecular Weight Distributions

David K. Potter† and A. Rudin*

Guelph–Waterloo Centre for Graduate Work in Chemistry, Department of Chemistry, University of Waterloo, Waterloo, Ontario, Canada N2L 3G1

Received October 20, 1989; Revised Manuscript Received June 21, 1990

ABSTRACT: Control of the shear history of some thermoplastics allows for modification of processing properties without changes in molecular weight distribution. Similar effects can be achieved by recovering polymers from solution under controlled conditions. In this study narrow molecular weight distribution polystyrenes were precipitated from chloroform solutions and dried. Residual solvent was present only in trace quantities, and there was no change in molecular weight distribution for any sample. Large variations were observed in the mean molecular weight between entanglements and in the zero-shear viscosity. The steady-state compliance was not affected by sample history. Trends predicted by reptation scaling laws were indeed observed, but the data for all the samples did not fit a unique curve. The data could be resolved into a single plot by using a modification of the theory of Kavassalis and Noolandi. It is concluded that the prior treatment of the polymer altered the entanglement spacing as well as the nature of the entanglements. This appears to be the first test of modern reptation theories in which both the molecular weights and entanglement spacings of the polymers could be varied.

Introduction

Experiments in which the polymer molecular weight was varied (by choice of sample) and in which the mean entanglement spacings of the samples could also be varied would provide a unique test of current reptation model theories, which predict the dependence of zero-shear viscosity on entanglement spacing and molecular weight. We report the results of such experiments here.

The average molecular weight between chain entanglements, M_e, has been estimated for a number of species of narrow dispersity polymer melts.[1] The quantity is often calculated by use of eq 1,[1-3] where G_N is the plateau modulus, ρ is the density of the material at temperature T, and R is the ideal gas constant:

$$M_e = \rho RT/G_N \quad (1)$$

The plateau modulus here is the value of shear modulus associated with the rubbery plateau region of the modulus–time spectrum, where the decay of the modulus is temporarily inhibited by the entanglement network of the sample. It is observed in stress relaxation experiments when the time scale of the experiment is short enough and when the polymer molecular weight is high enough to allow formation of an entanglement network.

Viscosity data, as a function of molecular weight, are another manifestation of an entanglement network, for narrow fractions of various polymers. These data show a change in slope of the bilogarithmic viscosity–molecular weight curve, from approximately 1 to 3.4, at some characteristic molecular weight, M_c. M_c is approximately related to M_e by a factor of 2.[1-3] For narrow fractions, the physical manifestations of an entanglement network do not appear at molecular weights less than this value.

The most probable condition of a macromolecule will be that in which it is entangled with its neighbors.[4] Conditions that allow diffusion of polymer segments for a sufficient period of time will ultimately result in the attainment of the most probable state. One could refer to this condition as the "equilibrium" entanglement state. This is the regime in which most of the measurements on narrow fractions have apparently been carried out.

Studies[1-3] of undiluted polymer fractions of various species show that, for sufficiently high molecular weights, the plateau modulus is a species-dependent property that is independent of polymer chain length. Although the entanglement spacing, of polymers with sufficiently large molecular weights, may be only species-dependent in the equilibrium entanglement condition, there is a substantial body of literature that indicates that this is not the case for samples that have not been allowed to equilibrate. Phenomenological studies[4-15] of melt elasticity and viscosity imply that the entanglement spacing, and therefore the plateau modulus, is also history dependent. Large variations in elasticity and/or viscosity are observed when samples are sheared or annealed or when they are precipitated out of dilute or concentrated solutions.

This result is of particular significance when characterizing commercial polymers because these materials will seldom be found in the "equilibrium" condition as a result of their various methods of production and processing. In this case, the properties of a polymer could conceivably be altered whenever a polymer is mechanically processed. Shearing the polymer to reduce elasticity and viscosity has been used to their advantage by industrial processors of thermoplastics to enhance the processability of polymer melts. Use of mechanical shearing to accomplish these ends has become known as "shear modification" or "shear refining".[4] Examples of commercial applications of the technique include the reduction of haze in polyethylene films, improvements in high-speed processing, increases in the processing rates at which the onset of processing defects occur, and alleviation of weld line problems.[4]

Solution modification, i.e., precipitation of the polymer out of dilute or concentrated solutions, is a convenient way to study the effects of sample history in the laboratory. It is the technique employed in this study and has previously been observed[4,12-15] to induce phenomenological changes that parallel those in shear modification processes.

The present work focuses on property changes that result from solution modification of polystyrenes. It is likely that property changes that result from the abrupt precipitation of polymers out of solutions of various concentrations result from the "trapping" of the macromolecules

† Present address: Tremco Ltd., Research and Development, 220 Wicksteed Avenue, Toronto, Ontario, Canada M4H 1G7.

0024-9297/91/2224-0213$02.50/0

of these samples in a nonequilibrium entanglement condition. Measurements of the entanglement spacings of such samples, along with the corresponding physical properties, should lead to an understanding of how these properties are affected by changes in the average entanglement spacing.

Physical properties measured in this work, besides the plateau modulus, include the glass transition temperature of the polymer, the zero-shear viscosity, and the steady-state compliance. These properties have been extensively studied[1] for polystyrenes in the equilibrium entanglement condition.

Specifically, the glass transition temperature of polystyrene becomes independent of molecular weight above a molecular weight of approximately 50 000 for narrow distribution polystyrenes. The limiting value of the glass transition temperature for polystyrene, after correcting for heating rate, has been reported to be 100 °C by several investigators.[1] Previous studies of solution modification of polystyrene have demonstrated that the glass transition temperature of this polymer is influenced, however, by its previous solution history.[12,13]

Above the critical molecular weight, M_c, the zero-shear viscosity for well-annealed polystyrenes, at equal friction coefficient, is proportional to the 3.4 power of molecular weight. Some investigators[16-25] have extended this relation to broad molecular weight distribution samples by correlating the viscosity with the weight-average molecular weight, M_w. The initial choice of this average was somewhat arbitrary,[16] and some workers have even questioned as to whether any particular molecular weight average should be uniquely correlate with melt viscosity.[17] Significant departures from the 3.4 power law are often hard to detect because viscosity–molecular weight data are usually presented by using bilogarithmic plots. Some data have appeared[17] that suggest a curved rather than a straight-line relationship for polydisperse polystyrenes. Nevertheless, the dependence of zero-shear viscosity on molecular weight appears to be reasonably represented by a 3.4–3.7 power law for molecular weights greater than about 40 000.

Limiting behavior is also observed[1,2,21,22,26-29] in the steady-state compliance of well-annealed narrow distribution polystyrenes when the molecular weight is greater than the critical molecular weight, M_c', which is approximately related to M_e by a factor of 6 or 7.[1,2] It has been postulated that this limiting behavior is also a manifestation of the entanglement network of the sample. The sensitivity of this parameter to polydispersity is also well-known.[3]

This paper is the first in a series of articles dealing with the properties of solution-modified polystyrenes. In this study, properties of narrow molecular weight distribution polystyrenes that have been subjected to solution treatment are examined. Property changes in these samples will not be complicated by the added variable of polydispersity.

Future publications will deal with solution treatment induced property changes in blends of polystyrene narrow fractions and property changes in broad distribution commercial polystyrenes.

Experimental Section

Five narrow-dispersity ($M_w/M_n < 1.2$) polystyrene standards were selected for study. Molecular weights are listed in Table I. All species have molecular weights greater than the critical molecular weight for entanglement coupling, M_c = 40 000, for polystyrene.[1]

Table I
Molecular Weight, Residual Solvent Content, and Glass Transition Temperatures of Solution-Modified Polystyrene Standards

sample	precipitation concn, g/L	mol wt	residual chloroform, wt %	glass transition temp, °C
09000		90 000	0	97.1
09005	5	90 000	0.0015	100.1
09010	10	90 000	0.0017	102.0
09020	20	90 000	0.0028	101.8
09050	50	90 000	0.0023	102.6
20700		208 000	0	99.3
20705	5	208 000	0.0028	101.8
20710	10	207 000	0.0024	102.1
20720	20	208 000	0.0006	100.6
20750	50	208 000	0.0012	101.9
49800		498 000	0	101.3
49805	5	498 000	0.0002	102.6
49810	10	498 000	0.0001	101.1
49820	20	498 000	0.0001	103.6
49850	50	498 000	NQ[a]	101.0
60000		600 000	0	101.3
60005	5	600 000	0.0001	101.7
60010	10	600 000	0.0002	100.9
60020	20	600 000	0.0002	102.4
60050	50	600 000	0.0018	101.0
90000		900 000	0	100.8
90005	5	900 000	0.0002	102.6
90010	10	900 000	0.0002	102.6
90020	20	900 000	0.0003	102.8
90050	50	900 000	0.0003	102.4

[a] NQ = residual solvent was detectable but not quantifiable.

Chloroform solutions of concentrations 5, 10, 20, and 50 g/L were prepared for each of the different molecular weight samples. The polymer was precipitated from these solutions by the abrupt addition of ethanol while stirring. The ethanol/chloroform volume ratio was 2:1. The stirrer speed was approximately constant for a given concentration. Agitation was continued until the precipitated polymer coagulated, leaving a clear solvent mixture. The polymer was then recovered by suction filtration and dried in a vacuum oven at 40 °C for a minimum of 6 weeks.

During the 6-week period the recovered samples were pulverized in a mechanical grinder, at liquid-nitrogen temperature, to facilitate residual solvent removal and to produce samples that were physically convenient to work with. The residual solvent content of all of the samples was measured by gas chromatography at 130 °C. Solutions of 1.5% (w/w) polystyrene in 1,2,4-trichlorobenzene were injected into columns (composition: 10% Carbowax 20M TPA on Chromosorb W, 80–100 mesh) fitted with a glass-wool plug to prevent column fouling due to polymer. The carrier gas was helium. The column eluent was detected by flame ionization. Size-exclusion chromatography (SEC), at room temperature, was used to measure molecular weight distributions, before and after solution and mechanical treatment. The SEC solvent was tetrahydrofuran. A UV detector recorded the eluting species as measured at a wavelength of 254 nm.

The glass transition temperature of the dried polymers were measured by differential scanning calorimetry (DSC). Apparent glass temperatures were recorded at heating rates of 5, 10, 15, and 20 °C/min and extrapolated to 1 °C/min values for all samples. Glass transition values are believed to be valid to ±0.5 °C.

A Rheometrics mechanical spectrometer, Model 605, was used to collect dynamic mechanical and stress relaxation data with parallel-plate geometry for all of the samples. Samples were molded at temperatures up to 240 °C while jogging the top tool to exclude air. In both types of test, the applied strain was 5%, which is well within the linear viscoelastic response region for all of the samples. Measurements were made under a nitrogen atmosphere to minimize possible sample degradation. Dynamic mechanical data were collected at frequencies between 10^{-2} and 1 rad/s for temperatures between 125 and 215 °C. Stress relaxation data were collected at 170 °C. The step time, which is the time required to achieve full imposition of the test strain, was of the order of 10^{-2} s.

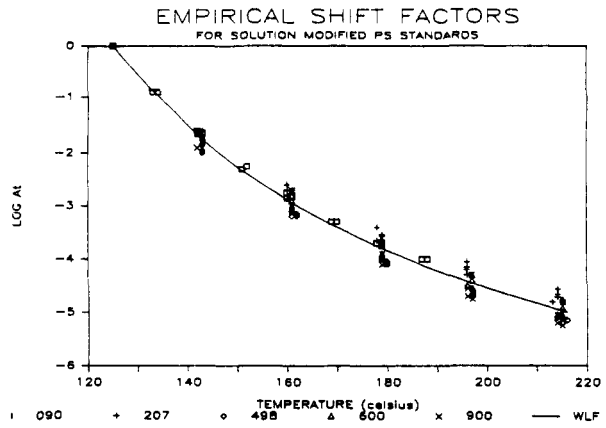

Figure 1. Empirical shift factors for all of the polystyrene narrow fractions studied. The solid line is a nonlinear least-squares fit of the WLF equation to the data.

Repeated experiments on already measured specimens produced duplicate results, indicating that no significant annealing took place during the measurements.

Results and Discussion

Molecular Weight and Residual Solvent Analysis. The SEC chromatograms (supplementary material available) for the solution-modified polystyrene standards and the original polymer were the same. Solution treatment has not altered the molecular weight distribution for any of the standards.

Table I lists the samples and the results of the residual solvent analysis by GC. Samples are coded according to molecular weight and the solution concentration from which the material was precipitated. The first three numbers in each sample code represent the molecular weight in thousands, and the last two numbers reflect the solution concentration in grams per liter. Residual ethanol was detected, but the quantities were too small to be quantifiable with our equipment. The weight percent chloroform listed in Table I is also very small and is unlikely to influence any physical properties.

Also listed in Table I are the glass transition temperatures for the polymers, before and after solution treatment. The "as-received" samples were not annealed, and some of these display T_g values that differ from those normally observed for polystyrene. The effect of residual solvent on T_g should lead to a decrease[1,30] in the glass transition temperature. In all cases here the glass transition temperature increased or remained the same as that for the original polystyrene.

Mechanical Data Analysis

Master Curve Construction and Comparison. Frequency shift factors were estimated empirically from both the storage and loss modulus data for all samples. This was done by using a computer to simultaneously plot storage and loss modulus data, for different temperatures and choosing values of the shift factor until good superposition was obtained between data for both moduli at different temperatures. The reference temperature was 125 °C. Modulus values were corrected for the temperature dependence of density by using the standard correction factor, $b(T) = \rho_0 T_0/\rho T$, where ρ is the density at temperature T and the subscripted values refer to the reference condition. Densities were estimated from[31] $\rho = -4.97 \times 10^{-4} T + 1.075$, which is independent of molecular weight for the molecular weight range studied here.

The logarithm of the empirical shift factors is plotted against temperature in Figure 1. No discontinuity is

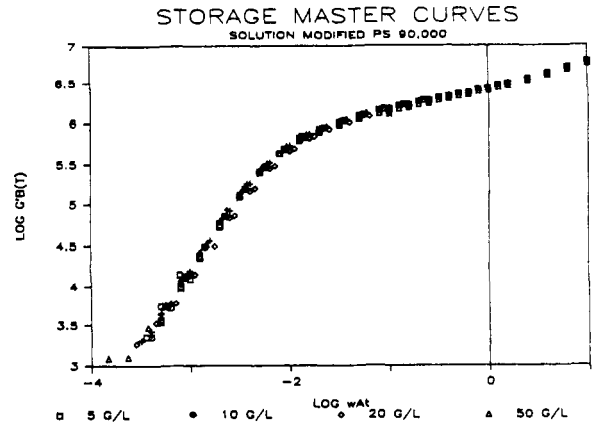

Figure 2. Storage modulus master curves for the 90 000 molecular weight samples of identical molecular weight distribution but different solution-precipitation histories.

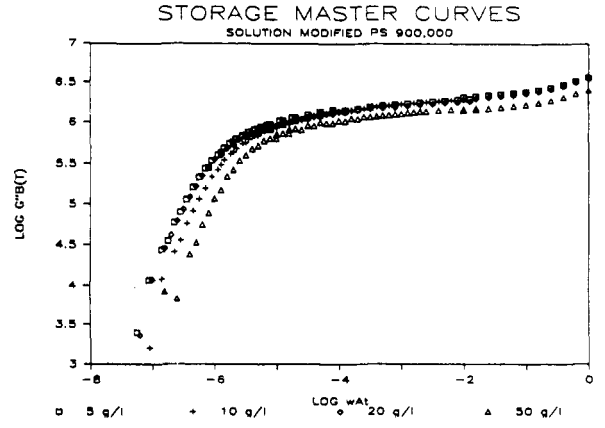

Figure 3. Storage modulus master curves for the 900 000 molecular weight samples of identical molecular weight distribution but different solution-precipitation histories.

apparent in the log a_t–temperature plot. A nonlinear least-squares algorithm was used to fit the data to the WLF equation[1,32] and estimate the WLF parameters. The line fitting of the data in the plot is described by eq 2. The

$$\log a_t = \frac{-9.3(T - T_0)}{(77 + T - T_0)} \tag{2}$$

friction coefficients of the samples differ, since they have different glass transition temperatures. The ratio of friction coefficients for the same sample at different temperatures appears not to vary significantly from sample to sample, since a common value of a_t fits the data.

Good time–temperature superposition of the data was achieved, as can be seen from the presented master curves (Figures 2–5; supplementary material available). Figures 2 and 3 are examples of storage modulus master curves, and Figures 4 and 5 are examples of loss modulus master curves focusing on the terminal peak in G''. The data in each plot are for samples having identical molecular weight distributions that have been recovered from solution at the four concentrations mentioned above.

Solution treatment has resulted in differences in some of the storage modulus curves and not in others. The 90 000 molecular weight sample exhibit the smallest (almost imperceptible) change in elastic response as a result of the solution treatment conditions used here (Figure 2). With the other samples, some of the modulus curves for different concentrations overlap and others show some change in response (for example, Figure 3).

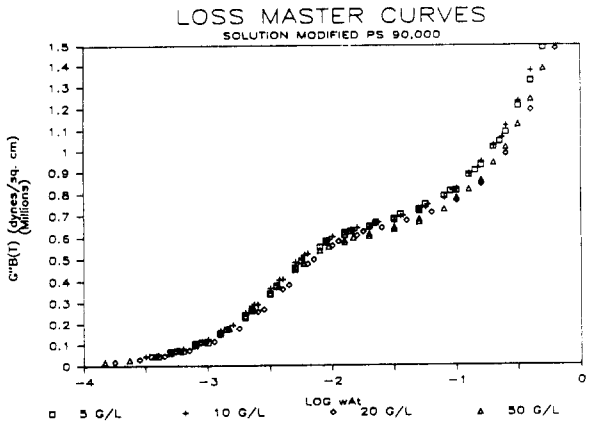

Figure 4. Loss modulus master curves for the 90 000 molecular weight samples of identical molecular weight distribution but different solution-precipitation histories.

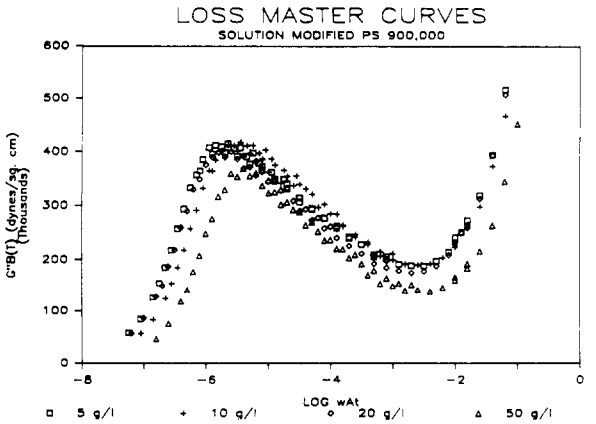

Figure 5. Loss modulus curves for the 900 000 molecular weight samples of identical molecular weight distribution but different solution-precipitation histories.

Differences between samples with different solution histories are more apparent in the loss modulus plots. This is partly because these plots are linear rather than logarithmic along the modulus axis. The 20 and 50 g/L curves diverge from the 5 and 10 g/L curves with increasing frequency for the 90 000 molecular weight sample (Figure 4), in which differences are barely observable in storage modulus plots. Solution treatment has produced differences in the loss modulus spectrum for all of the samples studied (for example, Figure 5).

There does not appear to be any consistent pattern between the relative values of storage or loss modulus and the concentration of the solution from which the polymer was precipitated. If entanglement spacings of the recovered polymer were strictly a reflection of the degree of coil overlap in solution, then polymers precipitated from higher concentrations should exhibit the macroscopic manifestations of a more entangled macromolecular matrix than the corresponding lower concentration analogues. The fact that no pattern is observed likely relates to the conditions of precipitation. Stirring was necessary to facilitate fast mixing of solvent and nonsolvents so that precipitation would occur abruptly. The degree of overlap of the polymer coils in solution will be influenced by the speed of stirring and the shear stress field to which the polymer is subjected in solution.

Shearing a polymer solution, of sufficient concentration, has long been known[33] to lead to a hysteresis in solution physical properties attributable to temporary alteration of the polymer solution network. Abrupt precipitation of the polymer under these different conditions will not yield

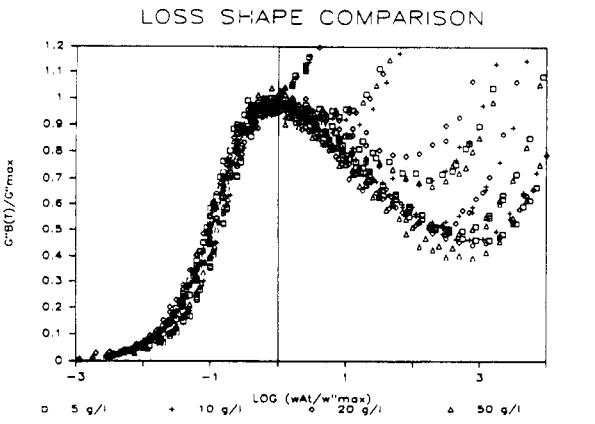

Figure 6. Loss modulus master peaks, for all of the samples studied here, that have been normalized with regard to the peak maximum and the frequency at which the maximum occurs. Solution treatment has not altered the shape of the loss peak for any of these samples.

an entanglement network that reflects coil overlap in quiescent solutions at the particular concentration. The stirring speed was not rigorously controlled here and variations in this parameter could also alter the relative rankings of network modification.

In any event, our objective here was not primarily to study the effects of concentration on polymer coil overlap but to demonstrate that polystyrenes can exist in various rheological states and to show that these different behaviors can be rationalized with the aid of modern theoretical concepts.

It is apparent that solution treatment has altered the loss modulus master curves in the magnitude of modulus response and, in some cases, by a slight shift in the frequency axis. The effect of solution treatment on the shape of the loss peak is not easily discernable from the master curves alone. The effect of solution treatment on the shape of the loss peak in G'' can, however, be observed by reducing the data in terms of the maximum in G'' and the frequency at which the maximum occurs.[2] Figure 6 is a plot of $G''B(T)/G''B(T)_{max}$ versus $\omega a_t/\omega a_{t\,max}$ for all of the recovered polymers. Except for some displacement of the 90 000 molecular weight samples, and the usually observed[2,34] network dependent rise to the transition zone on the transition side of the loss peak, all of the loss spectra can be seen to overlap within what can be considered reasonable error in the selection of maximum values from the measured data points rather than by curve fitting. The largest error resulting from maxima determination occurs with the 90 000 molecular weight samples because no maximum is observed in these spectra and the location of where the maxima would be expected in the absence of transition zone interference is subject to guess. In view of this evidence, we conclude that solution treatment has not altered the shape of any of the loss peaks.

Estimation of Plateau Modulus. The plateau modulus is the value of modulus associated with the rubbery plateau region of the stress relaxation modulus–time curve or the dynamic storage modulus–frequency survey. However, direct measurement of the plateau modulus from such data can be subjective because modulus values in this region are often not constant as a function of time or frequency and a sloped curve is observed. Other methods[1] are therefore commonly used to estimate the plateau modulus to try and remove some of this subjectivity. One of the more common[1-3] of these methods involves the use of the phenomenological theory of linear viscoelasticity to obtain the plateau modulus from loss modulus data when a well-defined loss peak is observed.

Table II
Results of Four-Parameter Power Law Fit

sample	$A1$, $\times 10^{-4}$	$B1$, $\times 10^{-6}$	$A2$	$B2$
09005	46.0	0.060	1.68	0.744
09010	46.2	0.051	1.76	0.753
09020	31.6	0.160	1.58	0.711
09050	48.7	0.024	1.51	0.770
20805	16.0	0.136	1.33	0.716
20810	15.9	0.156	0.965	0.709
20820	13.4	0.191	1.59	0.712
20850	15.1	0.164	1.69	0.722
49805	6.98	0.179	2.21	0.688
49810	10.0	0.126	2.53	0.708
49820	9.30	0.133	2.53	0.699
49850	8.15	0.133	1.80	0.704
60005	5.99	0.177	2.50	0.694
60010	5.90	0.180	2.39	0.693
60020	5.11	0.195	2.25	0.697
60050	4.80	0.181	2.06	0.692
90005	6.11	0.155	2.92	0.697
90010	5.90	0.166	2.56	0.690
90020	4.89	0.173	3.02	0.697
90050	3.54	0.200	1.97	0.695

The plateau modulus, G_N, was estimated from the terminal peak in G'' by using eq 3, which involves measuring the area under this peak[1,3]

$$G_N = \frac{2}{\pi}\int_{\infty}^{-\infty} G''(\omega)\, \mathrm{d} \ln \omega \qquad (3)$$

where ω is the test frequency.

This method requires separation of the higher frequency terminal response in G'' from the response in the transition zone with which it is overlapping. Following Colby's Ph.D. dissertation,[35] the assumption was invoked that G'' data in the transition region and the transition side of the terminal region could be described by the sum of two power laws as follows.

$$G''(\omega a_t) = A1(\omega a_t)^{-B1} + A2(\omega a_t)^{B2} \qquad (4)$$

$$\text{for } 3(\omega a_t)''_{\max} < \omega a_t < 10^8 \text{ rad/s}$$

$$\text{dimensions} \qquad m/t^2 l = (m/t^{2+B1} l)t^{B1} + (m/t^{2-B2} l)t^{-B2}$$

Data between 3 times the frequency at which the maximum in G'' occurs and 1 rad/s were fitted to the above equation using a nonlinear least-squares routine. The estimated parameters can be found in Table II.

It has been suggested[1] that the exponent describing the transition response in G'' (i.e., $B2$) should be independent of molecular weight and polymer type. The $B2$ values in Table II are indeed constant for the higher molecular weight species studied (i.e., 600 000 molecular weight and higher values). There is a slight increase in the value of $B2$ with the lower molecular weight samples. Since the region of terminal and translational overlap is better defined for species of higher molecular weight, and because of the limited transitional frequency range that we are fitting, it is likely that our estimate of the transitional exponent, $B2$, is being influenced by contributions from the terminal region in the lower molecular weight samples. We therefore average the values of $B2$ for molecular weights 600 000 and 900 000 and obtain a value for $B2$ of 0.694 for polystyrene. This value is in good agreement with a value of 0.67 reported for polybutadiene.[35]

Table III contains values of the power law coefficients when the data is fit with eq 4 at a constant value of $B2$ = 0.694. The value of the preexponential coefficient, $A2$, appears to be varying randomly with molecular weight. It has been suggested elsewhere[1] that this parameter is molecular weight independent. Variations in $A2$ were not averaged out in this treatment because the samples are not in the "equilibrium entanglement condition", and comparison of the master curves reveals a shift in the frequency location of the transition region for some of the samples. This shift cannot be attributed to error in the time–temperature superposition analysis because the data in this region were collected at the reference temperature and have not been WLF frequency shifted.

Table III
Results of Three-Parameter Power Law Curve Fit with $B2 = 0.694$

sample	$A1$, $\times 10^{-4}$	$B1$, $\times 10^{-6}$	$A2$
09005	35.5	0.120	1.78
09010	32.5	0.136	1.89
09020	28.5	0.188	1.61
09050	32.8	0.120	1.66
20805	14.0	0.165	1.35
20810	14.7	0.172	0.976
20820	11.5	0.222	1.61
20850	11.8	0.210	1.71
49805	7.49	0.169	2.21
49810	8.95	0.139	2.53
49820	8.86	0.139	2.53
49850	7.61	0.141	1.80
60005	5.99	0.177	2.50
60010	5.90	0.180	2.39
60020	5.11	0.195	2.25
60050	4.80	0.181	2.06
90005	6.11	0.155	2.92
90010	5.90	0.166	2.56
90020	4.89	0.173	3.02
90050	3.54	0.200	1.97

Table IV
Results of Two-Parameter Power Law Curve Fit with $B2 = 0.694$ and $B1 = 0.33$

sample	$A1$, $\times 10^{-4}$	$A2$, $\times 10^{-6}$	sample	$A1$, $\times 10^{-4}$	$A2$, $\times 10^{-6}$
09005	19.0	2.00	49820	2.03	2.66
09010	18.8	2.07	19850	1.65	1.91
09020	19.7	1.72	60005	1.51	2.54
09050	18.1	1.85	60010	1.55	2.48
20805	6.77	1.46	60020	1.65	2.32
20810	7.95	1.08	60050	1.23	2.13
20820	7.47	1.68	90005	0.904	3.02
20850	7.17	1.79	90010	1.12	2.67
49805	2.64	2.27	90020	0.959	3.10
49810	1.83	2.67	90050	0.969	2.02

A comparison of the terminal power law exponent, $B1$, with the coefficients of the four-parameter curve fit reveals some change in $B1$ for samples lower than 600 000 in molecular weight. It would seem that this parameter is also being influenced by the molecular weight dependent resolution of the terminal peak. It has been suggested[35] that the value of the exponent in this region should be molecular weight independent, as well, and that a limiting value of $B1$ should be observed for high molecular weights. A recent study,[35] with polybutadiene fractions, used molecular weights high enough to observe limiting behavior in $B1$, and the limiting value observed was −0.33. This has apparently been observed with other polymers as well. The molecular weights used in this study are not large enough to observe limiting behavior.

The limiting value of $B1 = 0.33$ was therefore assumed, and a two-parameter curve fit with $B2 = 0.694$ was performed. The values of $A1$ and $A2$ can be found in Table IV. The value of $A1$ is expected to be molecular weight dependent (the height of the terminal peak is molecular weight dependent). Figure 7 is a bilogarithmic plot of $A1$ versus molecular weight. The line fitting of the data was obtained by linear least squares and has a linear least-squares correlation coefficient of −0.994. This leads

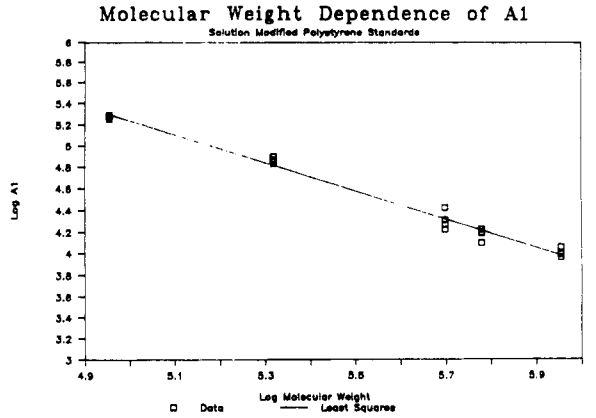

Figure 7. Molecular weight dependence of the terminal coefficient $A1$. The solid is a least-squares fit. The coefficient is independent of solution treatment.

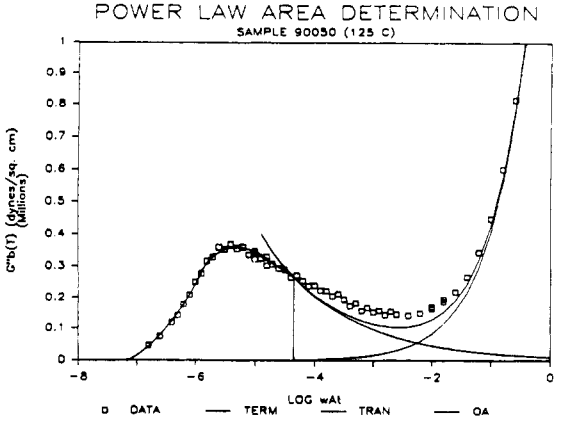

Figure 8. Power law curve fit to the data for sample 90050. The terminal power law curve intersects the data at the line perpendicular to the abscissa. The area under the data to the right of the perpendicular line was determined by numerical integration. The area under the data to the left of the line was determined by planimetry.

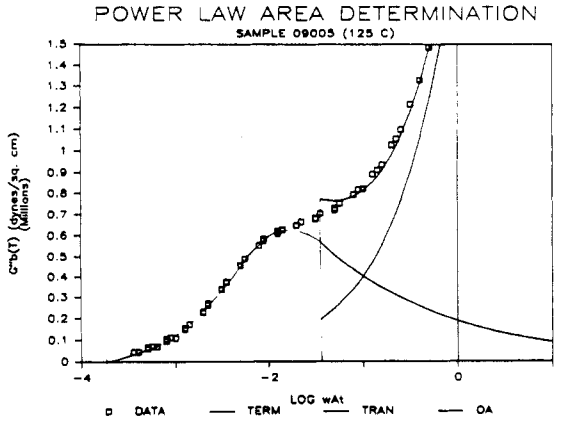

Figure 9. Power law curve fit to the data for sample 09005. In this case the terminal power law curve does not intersect with the data. The line perpendicular to the abscissa is at a frequency of $3\omega a_t$. The curve from $3\omega a_t$ to the data is an interpolation done by hand. The area under the terminal power law curve, to the right of the perpendicular line, was determined by numerical integration. The area to the left of the perpendicular line was determined by planimetry.

to the conclusion that the terminal zone, for $\omega a_t > 3\omega a_t P_{max}$, can be described by eq 5 for polystyrene at 125 °C. Our resolution of the terminal peak is independent of prior sample history.

$$G''(\omega a_t)_{terminal} = 7.4 \times 10^{11} M^{-1.3} \omega a_t^{-0.33} \quad (5)$$

Table V
Rheological Parameters of Solution-Modified Polystyrene Standards

sample	G_N (125 °C), 10^{-6} dyn/cm^2	η_0 (170 °C), 10^{-5} P	ζ_0 (170 °C), 10^6 dyn·s/cm	$J_e°$ (125 °C), 10^6 cm^2/dyn
09005	1.82	1.1	1.22	1.0
09010	1.78	1.1	1.51	1.0
09020	1.73	1.1	1.47	1.0
09050	1.71	1.1	1.61	1.0
20805	1.29	11	1.47	1.6
20810	1.33	12	1.52	1.6
20820	1.41	13	1.29	1.6
20850	1.42	14	1.49	1.6
49805	1.36	300	1.61	2.0
49810	1.29	310	1.36	2.0
49820	1.21	210	1.81	2.2
49850	1.06	310	1.35	2.2
60005	1.44	1200	1.46	1.4
60010	1.33	1000	1.33	1.6
60020	1.28	980	1.58	1.6
60050	1.18	810	1.35	1.6
90005	1.36	2200	1.61	1.6
90010	1.44	2100	1.61	1.5
90020	1.35	1900	1.65	1.6
90050	1.13	1700	1.58	1.6

Table VI
Molecular Parameters of Solution-Modified Polystyrene Standards Calculated from Rheological Measurements

sample	M_e (170 °C)	$N+1$ (170 °C)	sample	M_e (170 °C)	$N+1$ (170 °C)
09005	20 000	5.8	49820	30 100	6.2
09010	20 500	6.1	49850	34 300	5.2
09020	21 000	6.1	60005	25 300	4.4
09050	21 300	6.2	60010	27 500	4.5
20805	28 200	6.4	60020	28 400	4.7
20810	27 500	6.3	60050	30 900	4.7
20820	25 900	5.9	90005	26 800	5.2
20850	25 700	6.0	90010	25 400	5.3
49805	26 900	5.5	90020	27 100	5.4
49810	28 200	5.2	90050	32 200	5.5

Figures 8 and 9 are G'' master curves for molecular weights 900 000 and 90 000, respectively. Also plotted are the power law curves from the curve fitting described above. The power law description shows reasonable coincidence with the data, for the 900 000 molecular weight sample. The terminal power law curve intersects with the data and a reasonable estimation of the plateau modulus can be obtained by integrating, from the point of intersection to high frequency, and adding the contribution from the area of the remainder of the loss peak, which can be determined by planimetry. The integration to high frequency was done by calculating the value of the integral for successive decades of frequency until the value of the integral changed by less than 0.5% between successive decades. This procedure was followed for samples having molecular weights 900 000–498 000.

The 90 000 and 208 000 molecular weight master curves were not intersected by the terminal power law curves (e.g., Figure 9). In these cases, the shape of the terminal response in G'' from $3\omega a_t$ to intersection with the data was interpolated by hand with due consideration for the shape of the terminal peak. Although some subjective error will be incurred with this procedure, the error should be minimal because the shapes of the loss peaks have not been altered by solution treatment.

Estimated plateau modulus values are listed in Table V. The average molecular weight between chain entanglements, M_e, can be calculated at 170 °C by using eq 1 because the plateau modulus is insensitive to temperature.[2] The M_e values can be found in Table VI. Plateau modulus values for the 90 000 molecular weight samples are much

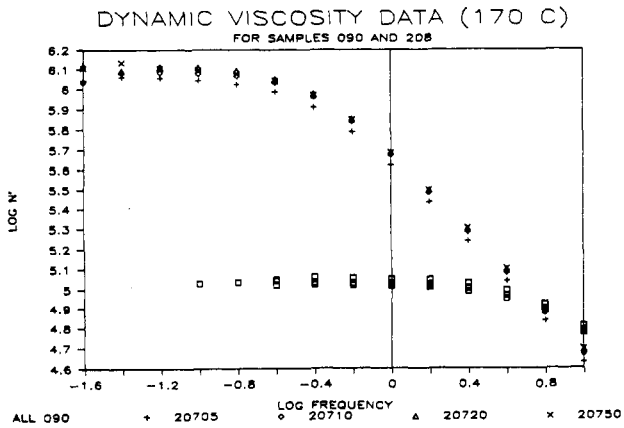

Figure 10. Dynamic viscosity data from which the zero-shear viscosity was estimated by using eq 7 for the 90 000 and 208 000 molecular weight samples.

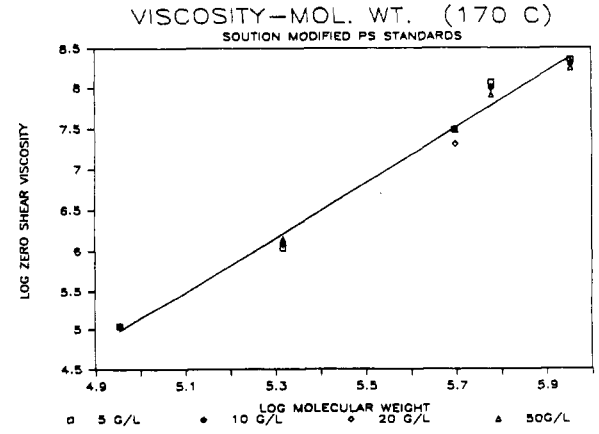

Figure 11. Dependence of zero-shear viscosity on molecular weight for the solution-treated polystyrenes. The solid line was obtained by least-squares fitting. It has the expected slope of 3.4.

larger than those for the other samples. This may be an artifact of the estimation method mentioned above since these samples have the least resolved loss peak. Values of plateau modulus for the other samples vary as much as 30%, with differences in solution-precipitation history.

Estimation of Zero-Shear Viscosity. The zero-shear viscosity of the higher molecular weight samples (498 000, 600 000, and 900 000 molecular weight) was estimated by using eq 6, which involves measuring the area under the stress relaxation modulus–time spectrum.[1]

$$\eta_0 = \int_0^\infty G(t)\,dt \tag{6}$$

Stress relaxation experiments did not yield reliable modulus–time data for molecular weights 90 000 and 208 000 at the test temperature (170 °C) because of the fast response time of these polystyrenes under these conditions. The zero-shear viscosity for these samples was obtained from dynamic mechanical frequency sweeps at 170 °C by using eq 7.[1]

$$\eta_0 = \lim_{\omega \to 0} \eta'(\omega) \tag{7}$$

Limiting behavior in the dynamic viscosity was observed for these lower molecular weight polystyrenes (Figure 10).

The zero-shear viscosities can be found in Table V. The viscosity values at constant molecular weight vary as much as 50%, depending on sample history. These differences are, however, not visually striking when a logarithmic plot of zero-shear viscosity versus molecular weight is constructed (Figure 11). Linear least squares fits a line with the expected slope of 3.4 to the data with a correlation coefficient of 0.994.

Estimation of Steady-State Compliance. The dynamic mechanical storage compliance, J', was used to estimate the steady-state compliance, $J_e°$, according to eq 8,[1] which requires limiting behavior in J' at low frequencies.

$$J_e° = \lim_{\omega \to 0} \frac{G'}{(G')^2 + (G'')^2} = \lim_{\omega \to 0} J' \tag{8}$$

Some difficulty is encountered, particularly with higher molecular weight samples, in ensuring that limiting behavior has been reached at low frequencies. Figure 12 is a bilogarithmic plot of J' against G'[25] for all of the samples studied. In each case the storage compliance falls into its low-frequency limit at relatively high values of G' so that the limiting values of J' are easily observable. The estimated values of $J_e°$ are listed in Table V.

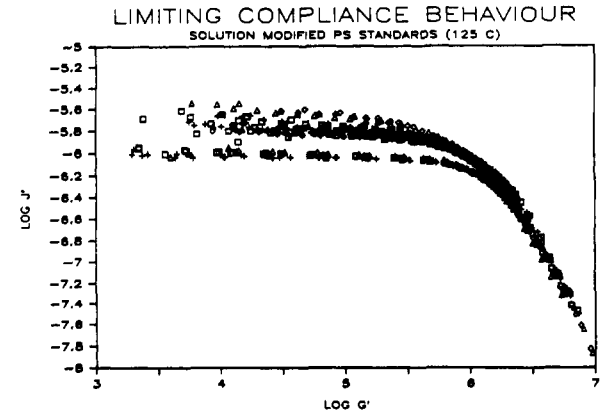

Figure 12. Limiting compliance behavior of solution-treated polystyrene standards. The lower data set are for the 90 000 molecular weight samples. Data for the 498 000 molecular weight samples reach limiting behavior at slightly larger compliance values than the other higher molecular weight samples.

For narrow fractions in the equilibrium entanglement condition, it has been established[1,2] that the steady-state compliance increases with molecular weight until a critical molecular weight, $M_c' = 6$ or 7 M_e, is reached. Beyond the critical molecular weight, $J_e°$ becomes molecular weight independent. This behavior has been attributed to the entanglement network of the material. It is also well-known[3] that $J_e°$ is very sensitive to polydispersity and particularly to the higher molecular weight tail of the molecular weight distribution.

One might expect that variation of the entanglement spacing of a sample, without changes to the molecular weight distribution, should be reflected in some variation in $J_e°$. This is not observed here. The values of $J_e°$ for samples of the same molecular weight show no variation with sample history. The expected[1,2] limiting behavior of $J_e°$ at high molecular weights is observed (Figure 13). The value of steady-state compliance for the 90 000 molecular weight samples is less than that for the higher molecular weight samples because a molecular weight of 90 000 is less than M_c'. The values of compliance for the other samples are approximately the same except for those of the 498 000 molecular weight samples, which appear to be slightly high. Assuming that the steady-state compliances of these samples also do not reflect variations in entanglement spacings as with the other high molecular weight samples, the slightly elevated compliance values may be due to the presence of a small amount of higher molecular weight material in the molecular weight distribution of

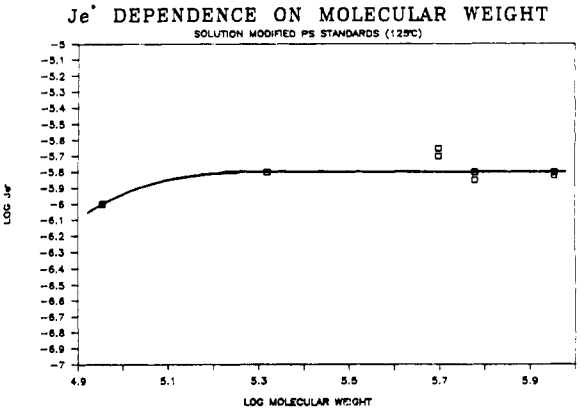

Figure 13. Dependence of the steady-state compliance on molecular weight. The usual limiting behavior of $J_e°$ as a function of molecular weight is observed. This parameter appears to be insensitive to sample history.

these samples. It has been previously[3] noted that $J_e°$ is extremely sensitive to higher molecular species in the molecular weight distribution that are not easily detected by size-exclusion chromatography.

It appears that any variation in $J_e°$ resulting from an alteration of the entanglement spacing in the samples is either nonexistent or too small to be detected with these measurements.

Entanglement and Viscosity

Reptation. Changes in zero-shear viscosity should be related to changes in entanglement spacings because entanglements will act as constraints to the motions of macromolecules in flow. Many models have been proposed to predict the relationship between viscosity and entanglement molecular weight. One of the more effective recent models is based on reptation theory.[36-40] According to this theory the zero-shear viscosity should scale as the cube of molecular weight divided by the square of the average molecular weight between chain entanglements (eq 9).

$$\eta_0 \sim M^3/M_e^2 \tag{9}$$

The present data provides a unique test of this prediction because both M and M_e weights are varied here, as opposed to conventional data collected with the polymer in the "equilibrium" entanglement state where the molecular weight between chain entanglements appears to be constant. It is convenient to remove the molecular weight dependence of viscosity to check the scaling prediction in terms of M_e, and this can be accomplished by plotting log (M^3/η_0) against log M_e^2. A straight line of slope 1 should be observed to satisfy the above relationship.

There is, however, another factor, that is normally a constant for standards in the "equilibrium" entanglement condition that should be accounted for here. Untreated standards will exhibit a convergence of modulus data in the transition region provided that molecular weights are sufficiently high. As previously pointed out, the transition regions for these samples do not all overlap. The position of the transition region is related to the monomeric friction coefficient that is experienced in the polymer matrix, and changes in this friction coefficient will result in proportional variations of the viscosity. A proper test of the scaling prediction in terms of M_e must therefore use a viscosity that is reduced not only in terms of the molecular weight effect but also in terms of any variation in friction coefficient.[1,2]

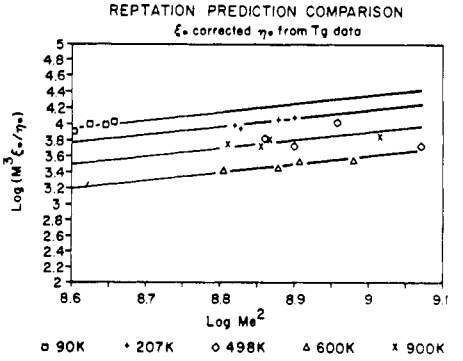

Figure 14. Test of the reptation model scaling prediction for the relationship between viscosity and the entanglement molecular weight. The molecular weight and friction coefficient dependencies of viscosity have been accounted for. Reptation behavior is depicted by a linear curve of slope 1 in this plot. The data show four lines of unit slope rather than the unique curve expected.

The change in friction coefficient for these samples, as compared to the equilibrium value, can be estimated from the observed change in the glass transition temperature. This is done by first calculating the shift factor, $a_{\Delta T_g}$, due to the change in T_g, using a modified form of the WLF[1] equation:

$$\log a_{\Delta T_g} = \frac{-C_{1,g}C_{2,g}(T_{g_1} - T_{g_2})}{(C_T + (T_{g_1} - T_{g_2}))C_T} \tag{10}$$

T_{g_1} and T_{g_2} are the glass transition temperatures before and after solution-precipitation treatment, $C_{1,g}$ = 13.7 K and $C_{2,g}$ = 50 K are the WLF parameters for polystyrene when the glass transition temperature is the reference temperature, and $C_T = C_{2,g} + T - T_{g_1}$, where T is the temperature of interest.

The monomeric friction coefficient of the treated polymer is related to that of the untreated polymer by eq 11.[1] $[\zeta_0]_{mod}$ is the monomeric friction coefficient for the

$$a_{\Delta T_g} = \frac{[\zeta_0]_{mod}}{[\zeta_0]_{equil}} \tag{11}$$

solution modified polymer, and $[\zeta_0]_{equil} = 1.21 \times 10^{-6}$ dyn·s/cm is the monomeric friction coefficient for polystyrene in the "equilibrium" entangled condition at 170 °C.[1] $[\zeta_0]_{equil}$ is independent of molecular weight since the samples used here are of sufficiently large molecular weight.

The monomeric friction coefficients estimated for the treated samples can be found in Table V. All values are larger than that for untreated samples, as expected, because all of the glass temperatures are higher than that of untreated polystyrene.

It is now possible to correct the viscosity data for the difference in friction coefficient, and Figure 14 is a bilogarithmic plot of $M^3\zeta_0/\eta_0$ against M_e^2. Rather than the expected linear curve of slope 1, there are four linear curves, all of slope 1. Although the basic reptation model predicts the correct scaling relation for each polystyrene, there appears to be some dependence of viscosity that is not accounted for by the entanglement spacing alone.

Figure 14 suggests that, at a given value of M_e, the value of zero-shear viscosity is enhanced from one set of samples to the next as one moves down the ordinate from one line to the next. A particular entanglement spacing size contributes more to the zero-shear viscosity of the samples

with lower reduced viscosities than for those of higher reduced viscosity.

It is important to remember that these differences are a result of sample history. No variation in polymer molecular weight has been observed as a result of solution-precipitation treatment. The comparison of the shapes of the loss spectra above indicates there has been no alteration in the distribution of relaxation times in the terminal region and this suggests that no change in the mechanism of relaxation has occurred. It appears, from the loss data, that only the magnitude of modulus response has been altered. One should expect that, after accounting for shifts in the transition zone and reducing the viscosity accordingly, a unique viscosity–entanglement molecular weight relationship would be observed. The fact that this is not seen leads to the speculation that solution modification has altered not only the magnitude of the entanglement spacing but perhaps the nature of the entanglement coupling itself.

Coordination Number Model. Recently, Kavassalis and Noolandi[41-43] have treated the entanglement problem using a statistical mean-field approach to the topology of polymer chains in the matrix. This model considers the number of other chains surrounding a test chain in a sphere having diameter, D_e, equal to the mean distance spanned by an entangled segment of N_e bonds with characteristic ratio, C_∞, and bond length, l (eq 12).

$$D_e = N_e^{1/2} C_\infty^{1/2} l \tag{12}$$

Specifically, the number of nontail chains (those that do not end with a tail in the sphere) is the only adjustable parameter in the model, which otherwise offers exact solutions. The average number of nontail chains (hereafter referred to as chains) in the test sphere represent a way of defining the nature of an entanglement coupling on a statistical basis. The number of neighboring chains in the test sphere, called the coordination number, can be viewed as the average number of chains that constitute a constraint to lateral motions of the test chain or the number of chains that, on the average, make up an entanglement coupling.

In the long-chain limit, the coordination number, $\bar{N}$, is expressed by eq 13. Here, ρ is the polymer density, C_∞ is

$$\bar{N} + 1 = \frac{\pi \rho C_\infty^{3/2} l^3}{6\mu_m} N_e^{1/2} \tag{13}$$

the characteristic ratio (the ratio of the end-to-end distance of a polymer molecule to the end-to-end distance of the random-walk model with the equivalent number of bonds), l is the bond length, μ_m is the monomer mass per skeletal bond, and N_e is the number of monomer units between chain entanglements. A survey of the literature data collected on narrow fractions for many polymers suggests that the coordination number is a constant for the "equilibrium" entanglement condition.[43]

The data presented in this work are not for polystyrenes in the equilibrium entanglement condition. Because of our precipitation process, it is possible that chain topologies have been introduced that do not conform to those in the equilibrium situation. The collapse of a polymer chain upon itself and some preservation of the end-to-end chain distance that existed during precipitation are examples of situations that are possible with these samples. We therefore refer to any coordination numbers that we derive from these data and the Kavassalis–Noolandi model as "effective coordination numbers".

The coordination number model has been derived strictly from considerations of chain topology in a static system. Analysis of our dynamic data using this model requires that we adopt models for dynamic behavior with incorporation of the coordination number scheme into the dynamic model.

A convenient dynamic model to use for this purpose is the modified Rouse model[44,45] for molecular weights greater than the critical molecular weight for chain entanglement. The modified Rouse model gives eq 14 for the zero-shear viscosity. N_0 is Avogadro's number, η is the density, a is

$$\eta_{0R} = \frac{\rho N_0 a^2 M Q_e \zeta_0}{36 M_0^2} \tag{14}$$

the root-mean-square end-to-end distance per square root of the number of monomer units, M is the polymer molecular weight, M_0 is the monomer molecular weight, ζ_0 is the monomeric friction coefficient, and Q_e is a numerical factor dependent on the number of entanglement loci per molecule. The reptation model scaling prediction can be built into the modified Rouse model equation by setting $Q_e = M^3/M_e^2$.

One can also recast eq 14, using eq 13, so that viscosity is expressed in terms of the coordination number rather than the entanglement molecular weight, M_e.

If eq 13 holds for our nonequilibrium samples, then the viscosities estimated using eqs 14 and 15 will be equal because the volume of the test sphere (via eq 12) will be dependent only on the entanglement molecular weight, M_e.

$$\eta_{0\ \mathrm{coord}} = \frac{\pi^4 \rho^5 C_\infty^6 l^{12} N_0 a^2 M^3 \zeta_0}{6^6 M_0^4 \mu_m^4 (\bar{N}+1)^4} \tag{15}$$

The application of the reptation model in the preceding section suggests that some difference exists between samples such that reduced viscosities do not follow a unique relationship with the entanglement molecular weight. We postulate that this additional viscosity dependence can be accounted for by considering variations of the coordination number, independently of M_e.

With the assumption that differences between the viscosity predicted by the eq 14 and that predicted by eq 15 are due to differences in the coordination number, eq 16 can be formulated to express the ratio of these two estimated viscosities in terms of M_e and the coordination number

$$\frac{\eta_{0\ \mathrm{coord}}}{\eta_{0R}} = \frac{K M_e^2}{(\bar{N}+1)^4} \tag{16}$$

where

$$K = \frac{\pi \rho^4 C_\infty^6 l^{12}}{6^4 M_0^2 \mu_m^4}$$

Equation 16 was used to calculate the values of "effective coordination numbers" for these samples. This was done by substituting the experimentally observed values of zero-shear viscosity for $\eta_{0\ \mathrm{coord}}$ and estimating η_{0R} using literature constants for polystyrene (ρ = 0.991 g/cm^3 at 170 °C, C_∞ = 9.4, $l = 1.54 \times 10^{-8}$, M_0 = 104, μ_m = 52) and the values of M, M_e, and ζ_0 for these samples. These values are listed in Table VI for the respective polystyrenes. Those samples having a higher viscosity at a given value of M_e can be seen to have lower effective coordination number values.

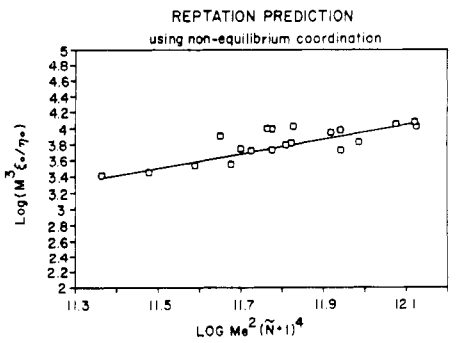

Figure 15. Test of a reptation scaling prediction expressed in terms of effective coordination numbers that are allowed to vary independently of the entanglement molecular weight for these nonequilibrium samples. A line of slope 1 depicts reptation dynamics. The data of Figure 13 reduces to a unique relationship when effective coordination numbers are taken into account.

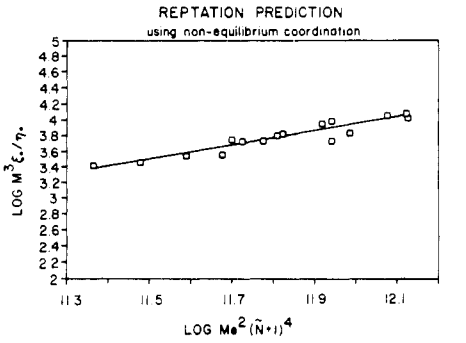

Figure 16. Same plot as Figure 14 except that the data for the 90 000 molecular weight samples, for which the estimation of M_e was the most uncertain, have been removed. The solid line was determined by least-squares fitting and has a slope of 0.95, which is close to the expected slope of unity for reptation dynamics.

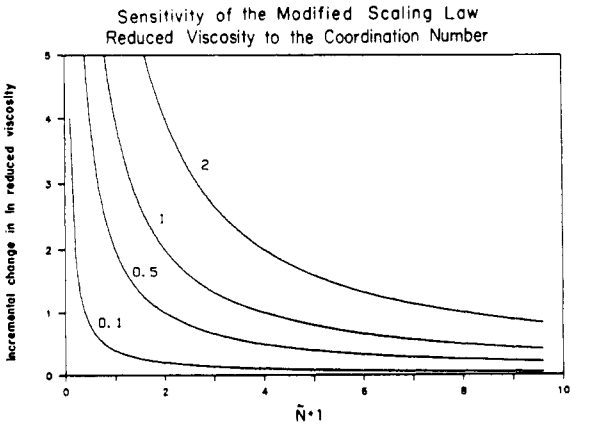

Figure 17. Sensitivity of the reduced viscosity to changes in the effective coordination number. The number above each of the curves corresponds to the change in effective coordination number for that curve.

The diameter of the test sphere, given by eq 12, can be expressed in terms of the coordination number by use of eq 13. The smaller the coordination number, the smaller will be the diameter, and therefore the volume, of the test sphere. This condition is consistent with the idea that a strand of molecular weight M_e is confined to a smaller volume. Since the volume is smaller, there will be fewer adjacent chains in the test volume. Viscosity is relatively higher than for other samples because the entanglement strand has less room available for segmental motion needed to slip its constraint.

We have chosen to generalize the Kavassalis–Noolandi model by introducing an "effective" topological constant for ease of computations. The model could have been generalized by introducing an "effective" characteristic ratio, for example. We chose not to do this because it is likely that a number of physical quantities are being altered by sample history and we have no measurements of these quantities.

It is worthwhile to note that this description of an alteration in the nature of the entanglement does not invoke any gross topological deformities to describe the nature of the couplings such as knots in the polymer chain. If such changes had occurred, it would be expected that changes in the dynamics of relaxation of the polymer chains should lead to a change in the shape of the loss peak, and this was not observed.

The reptation scaling prediction can be rewritten to accommodate our effective coordination number. The zero-shear viscosity scales as $1/M_e^2$, which is equivalent to $1/(\bar{N}+1)^4$ in the equilibrium case. When both parameters are treated as independent parameters for our nonequilibrium samples, scaling prediction eq 17 can be written

$$\eta_0 \sim \frac{M^3\zeta_0}{M_e^2(\bar{N}+1)^4} \tag{17}$$

As with the normally quoted analogue of this equation, a log–log plot of $M^3\zeta_0/\eta_0$ against $M_e^2(\bar{N}+1)^4$ should yield a straight line of slope 1. Unlike Figure 14, all data points should fall on the same line if our values of effective coordination number account for the differences between samples that produce different curves in Figure 14. Figure 15 is such a plot, and the data do fall roughly about the line, determined by least squares, of slope 0.91. It is interesting that the removal of points for which the determination of M_e was most suspect (the 90 000 molecular weight samples) leads to the line with a least-squares correlation coefficient of 0.93 and having slope 0.95 as depicted in Figure 16. This is very close to the expected slope of unity. We conclude that the effective coordination number scheme used here does adequately account for variations in viscosity as a result of solution modification.

It is desirable to know how sensitive the above scaling relationship is to the value of the effective coordination number. The sensitivity of the reduced viscosity, on a logarithmic scale, to the values of effective coordination number can be demonstrated by writing the scaling relationship as an equality, as in eq 18, and differentiating with respect to the coordination number. The constant "C" is assumed to be independent of the coordination number.

$$\ln\left(\frac{M^3\zeta_0}{\eta_0}\right) = \ln\left(M_e^2(\bar{N}+1)^4\right) + C \tag{18}$$

Figure 17 is a plot of the change in the increment of reduced viscosity as a function of $\bar{N}+1$ for different increments of coordination number. In the range of the effective coordination numbers estimated here (i.e., 4–7), variations of 0.5 in the effective coordination number result in a change of approximately half a decade in reduced viscosity. The reduced viscosity is evidently sensitive to the value of the effective coordination number, and small variations should be detectable even on bilogarithmic plots. The success of the model used here cannot therefore be due to the lack of sensitivity of the data to the measured values of the effective coordination number.

Speculation on the Morphology of Solution-Modified Polystyrenes. The implications of this analysis

are that solution modification can alter both the spacing between chain entanglements and the nature of the entanglement couplings. With the assumption that the effective coordination numbers correlate with the diameter of the test sphere, as in the equilibrium case, these data suggest that solution modification can result in a change in the average end-to-end distance of the polymer chain. Other physical processes are presumed to achieve this as well, such as the uniaxial stretching of polymer films or the spinning of polymer monofilaments.

A recent study[46] used small-angle neutron scattering to investigate the change in the macromolecular coil dimensions of amorphous polystyrene that had been oriented during solid-state coextrusion. Intensity contour plots clearly demonstrated that the spherical coil configuration of the macromolecules before extrusion had assumed an ellipsoid shape after extrusion. The longitudinal axis of the ellipsoid was oriented parallel to the direction of extrusion, and the transverse axis of the distorted coil was oriented perpendicular to the machine direction. The exact measurement of the longitudinal axis was not possible due to experimental difficulties and was estimated by assuming constant volume.

It seems likely that such orientation of the macromolecular coil would have an effect on the number of entanglements in which a given molecule would participate. It is also reasonable that oriented chains can pack into a smaller volume than those assuming a randomized "spaghetti" topology. Such packing should lead to a decrease in the volume per unit of mass that the molecule occupies. The number of surrounding chains that act as an "effective constraint" to macromolecular motion would presumably depend on the degree of orientation.

Studies[47,48] of iodine-tagged polystyrene in untagged polystyrene using electron microscopy showed that the segmental density distribution, across the polymer coil, was neither Gaussian nor symmetrical for individual molecules. Despite the casting of samples from dilute solution, the shape of the individual polystyrene macromolecules was not spherical either. However, averaging over many molecules in the sample, at several angles, a Gaussian density distribution and spherical molecular shape were obtained.

High-resolution, solid-state, ^{13}C NMR also revealed some local order[49] in amorphous polystyrene glasses. The extent and exact nature of the ordering were not known but the authors speculated that some segmental orientation would lead to increased efficiency in small-scale packing.

Others used[14,15] electron microscopy to investigate the morphology of solution-modified amorphous polystyrenes. These workers were able to detect some supermolecular structure in polystyrenes that had been solution treated.

Previous studies[4,12,13] of solution modification have indicated that the physical properties of the polymer return to their original values after annealing for a sufficient period of time. Such annealing would allow diffusion of polymer molecular segments, which would enable the macromolecule to once again assume the random-coil configuration that exists in the equilibrium case. Stretched films or spun monofilaments exhibit these same characteristics upon annealing as amorphous molecular segments diffuse to the less oriented random-coil configuration.

It would seem plausible to suggest, then, that abrupt precipitation of polystyrene from stirred solutions can result in a similar distortion in the shape of the macromolecular coil. This distortion would occur during the precipitation process in which the precipitating macromolecule would retain an elongation imparted to it by the shear field, generated by stirring, as it comes out of solution.

Confinement of macromolecular segments to a smaller volume is also supported by the change in glass transition temperatures of the samples in this study. If macromolecular segments were packed into a smaller volume than in the equilibrium case, a decrease in the available free volume would result. With less room for segmental motions associated with the glass transition to occur, an increase in the glass transition temperature is expected and has been observed here.

This study also demonstrates that rheological characterization of samples with a nonequilibrium entanglement network requires measurement of both the elastic and viscous responses of the material. For these samples, viscosity cannot be predicted solely from a knowledge of the microscopic elastic network spacings of the sample or, conversely, the elastic properties are not accessible strictly from a knowledge of viscosity. In the framework of the coordination number model, such interrelations require a fixed relation between the volume of the test sphere and the magnitude of the entanglement spacing. The equilibrium dependence will hold only when the polymer chain adopts the random-coil configuration.

Conclusions

Solution modification of polystyrene alters the entanglement spacing of the polymer as well as the nature of the entanglement coupling. For polystyrene standards, the dependence of zero-shear viscosity on molecular weight raised to the 3.4 power will give reasonable order of magnitude predictions in log–log representations.

Where more detailed accounting of polymer viscosity is needed, the relationship between viscosity and the magnitude of the entanglement spacing, as well as the nature of the entanglement coupling, must be investigated. Relationships between viscous and elastic response will not hold if the nature of the entanglement coupling is not taken into account. Rheological characterization of solution-modified samples will therefore require measurement of both the elastic response and the viscosity of the material.

The steady-state compliance of solution-treated polystyrenes unexpectedly demonstrates the same behavior as that observed for samples in equilibrium entanglement conditions. This parameter is unaffected by the changes in other material properties that are on the scale of those observed here.

A simple reptation model scaling prediction does not allow for variation in the nature of the entanglement coupling and so does not produce a unique relationship with all these samples. The coordination number model of Kavassalis and Noolandi[43] can be conveniently used to produce a reptation scaling relationship between viscosity and entanglement molecular weight if the nature of the entanglement coupling described by the model is allowed to become independent of the entanglement spacing. This implies that solution precipitation is altering the spatial dimensions of the polymer chains in the sample. This speculation is further supported by an observed increase in the glass transition temperature of these samples.

Acknowledgment. We thank the Natural Sciences and Engineering Research Council of Canada for financial support of this work.

Supplementary Material Available: Figures containing the SEC chromatograms of narrow molecular weight distribution, polystyrene standards before and after solution and mechanical

treatment, in each case of which these treatments have not resulted in a change to the polymer molecular weight distribution (Figures 1–5), storage modulus master curves, at 125 °C, for solution-treated polystyrene standards, in which each plot contains data for samples of identical molecular weight distribution but different solution-precipitation histories and the storage modulus curves differ as a result of previous history (Figures 6–8), and loss modulus master curves, at 125 °C, for solution-treated polystyrene standards, in which each plot contains data for samples of identical molecular weight distribution but different solution-precipitation histories and differences resulting from sample history are more apparent in these plots, partly because of the linear ordinate (Figures 9–11) (11 pages). Ordering information is given on any current masthead page.

References and Notes

(1) Ferry, J. D. *Viscoelastic Properties of Polymers*, 2nd ed.; John Wiley and Sons: New York, 1970.
(2) Graessley, W. W. *Faraday Symp. Chem. Soc.* **1983**, *18*, 7–27.
(3) Graessley, W. W. The Entanglement Concept in Polymer Rheology. *Advances in Polymer Science*; Springer-Verlag: New York, 1974; Vol. 16.
(4) Rudin, A.; Schreiber, H. P. *Polym. Eng. Sci.* **1983**, *23*, 422.
(5) Schreiber, H. P.; Rudin, A.; Bagley, E. B. *J. Appl. Polym. Sci.* **1965**, *9*, 887–892.
(6) Rokudai, M.; Fujiki, T. *J. Polym. Sci.* **1981**, *26*, 1427.
(7) Rokudai, M. *J. Appl. Polym. Sci.* **1979**, *23*, 463.
(8) Ajji, A.; Schreiber, H. P.; Rudin, A.; Teh, J. W. *J. Appl. Polym. Sci.* **1985**, *30*, 731.
(9) Teh, J. W.; Rudin, A.; Schreiber, H. P. *Plast. Rubber Process. Appl.* **1984**, *4*, 149.
(10) Teh, J. W.; Rudin, A.; Schreiber, H. P. *Plast. Rubber Process. Appl.* **1984**, *4*, 157.
(11) Pollett, W. F. O. *Br. J. Appl. Phys.* **1955**, *6*, 199.
(12) Ajji, A.; Carreau, P. J.; Rudin, A.; Schreiber, H. P. *J. Polym. Sci., Part B: Polym. Phys.* **1986**, *24*, 1983.
(13) Schreiber, H. P.; Ajji, A.; Yonming, L.; Rudin, A. Property Modifications in Polystyrene Recovered from Solution. *Current Topics in Polymer Science*; Ottenbrite, R. M., Utracki, L. A., Inoue, S., Eds.; Carl Hanser Verlag: New York, 1987; Vol. 2.
(14) Privalko, V. P.; Andrianova, G. P.; Besklubenko, Yu. D.; Narozhnaya, Ye. P.; Lipatov, Yu. S. *Vysokomol. Soedin.* **1978**, *A20* (No. 12), 2777–2783; *Polym. Sci. USSR* **1979**, *20*, 3114–3121.
(15) Andrianova, G. P.; Narozhnaya, Ye. L. *Vysokomol. Soedin.* **1975**, *A17* (No. 4), 923–928.
(16) Fox, T. G.; Flory, P. G. *J. Am. Chem. Soc.* **1948**, *70*, 2384.
(17) Rudin, A.; Chee, K. K. *Macromolecules* **1973**, *6*, 613.
(18) Ninomiya, K.; Ferry, J. D.; Oyanagi, Y. *J. Phys. Chem.* **1963**, *67*, 2297.
(19) Leaderman, H.; Smith, R. G.; Williams, L. C. *J. Polym. Sci.* **1959**, *36*, 233.
(20) Malkin, A. Y.; Blinova, N. K.; Vinogradov. G. V.; Zabugina, M. P.; Sabsai, O. Y.; Shalganova, V. C.; Kirchevshaya, I. Y.; Shatalov, V. P. *Eur. Polym. J.* **1974**, *10*, 445.
(21) Onogi, S.; Masuda, T.; Kitagawa, K. *Macromolecules* **1970**, *3*, 109.
(22) Akovali, G. *J. Polym. Sci., Polym. Phys. Ed.* **1967**, *5*, 875.
(23) Prest, W. M.; Porter, R. S. *Polym. J.* **1973**, *4*, 154.
(24) Montfort, J. P.; Marin, G.; Arman, J.; Monge, Ph. *Rheol. Acta* **1979**, *18*, 629.
(25) Struglinski, M. J.; Graessley, W. W. *Macromolecules* **1985**, *18*, 2630.
(26) Tobolsky, A. V.; Aklonis, J. J.; Akovali, G. *J. Chem. Phys.* **1965**, *42*, 723.
(27) Knoff, W. F.; Hopkins, I. L.; Tobolsky, A. V. *Macromolecules* **1971**, *4*, 750.
(28) Nemoto, N. *Polym. J. (Tokyo)* **1970**, *1*, 485.
(29) Mills, N. J.; Nevin, A. *J. Polym. Sci., Polym. Phys. Ed.* **1971**, *9*, 267.
(30) Jenckel, E.; Heusch, R. *Kolloid-Z.* **1953**, *130*, 89.
(31) Rudin, A.; Wagner, A.; Chee, K. K.; Lau, W. W. Y.; Burns, C. M. *Polymer* **1977**, *18*, 124.
(32) Williams, M. L.; Landel, R. F.; Ferry, J. D. *J. Am. Chem. Soc.* **1955**, *77*, 3701.
(33) Freundlich, H. *Thixotropy*; Hermann: Paris, 1935.
(34) Gotro, J. T. Doctoral Thesis, Northwestern University, 1983.
(35) Colby, R. H. Doctoral Thesis, Northwestern University, 1985.
(36) de Gennes, P.-G. *Scaling Concepts in Polymer Physics*; Cornell University Press: Ithaca, NY, 1979.
(37) Doi, M.; Edwards, S. F. *J. Chem. Soc., Faraday Trans. 2* **1978**, *74*, 1789.
(38) Doi, M.; Edwards, S. F. *J. Chem. Soc., Faraday Trans. 2* **1978**, *74*, 1802.
(39) Doi, M.; Edwards, S. F. *J. Chem. Soc., Faraday Trans. 2* **1978**, *74*, 1818.
(40) Doi, M.; Edwards, S. F. *J. Chem. Soc., Faraday Trans. 2* **1979**, *75*, 38.
(41) Kavassalis, T. A.; Noolandi, J. *J. Phys. Rev. Lett.* **1987**, *59*, 2674.
(42) Kavassalis, T. A.; Noolandi, J. *Polym. Prepr. (Am. Chem. Soc., Div. Polym. Chem.)* **1988**, *29* (1), 408.
(43) Kavassalis, T. A.; Noolandi, J. *Macromolecules* **1988**, *21* (9), 2869.
(44) Rouse, P. E. *J. Chem. Phys.* **1953**, *21* (7), 1272.
(45) Graessley, W. W. *J. Chem. Phys.* **1965**, *43*, 2696.
(46) Hadziioannou, G.; Wang, Li-H.; Stein, S. S.; Porter, R. S. *Macromolecules* **1982**, *15*, 880.
(47) Aharoni, S. M. *Macromolecules* **1978**, *11*, 677.
(48) Aharoni, S. M.; Kramer, V.; Vernick, D. A. *Macromolecules* **1979**, *12*, 265.
(49) Havens, J. R.; Koenig, J. L. *J. Polym. Sci., Polym. Lett. Ed.* **1983**, *21*, 243.

Registry No. Polystyrene, 9003-53-6.